

Simulations of a Demonstration of Cloud Albedo Change

S H Salter

Institute for energy systems, School of Engineering. University of Edinburgh.

E-mail: s.salter@ed.ac.uk

Abstract. The reflectivity of marine stratocumulus clouds can be increased by a change of the concentration of cloud condensation nuclei. The increase can be sufficient to reverse global warming Latham et (2008). This paper shows the results as a function of initial cloud conditions and spray quantity and shows that it may be difficult to detect planet saving effects by eye.

1. Introduction.

Twomey (1977) showed that the reflectivity of a cloud depends on the size distribution of its drops. For the same liquid water content, a large number of small drops will reflect more than a small number of large ones. For a wide range of cloud conditions, doubling the number of drops will increase reflectivity by about 0.056, Schwarz and Slingo (1996). In clean mid-oceanic clouds the concentration of cloud drops (set by humidity and the availability of condensation nuclei) is quite low, often between 50 and 100 per cm^3 Bennartz (2007) and sometimes as low as 10. The salty residues left after the evaporation of submicron drops of sea spray are ideal cloud condensation nuclei. Latham (1990) (2008) suggested spraying sub-micron drops of sea water into the marine boundary layer to increase the reflectivity of marine stratocumulus clouds and send more solar energy back out to space.

Figure 1 shows an artist's impression of a wind-driven spray-vessel which generates energy to make spray by dragging turbines through the water. Propulsion by Flettner rotors rather than conventional sails makes the system easier to control remotely. Figure 2 shows an estimate of the cooling power as a function of spray rate for a given set of initial conditions based on Twomey (1977). Design work on the sea going hardware and a possible spray generation system rated at 30 kg/sec of 0.8 micron drops is well-advanced, Salter et al. (2008).

This paper discusses a possible method to demonstrate to a non-technical decision-maker whether or not the system is working. The problem is that the change in cloud contrast needed to cancel the excess solar input predicted to result from double pre-industrial CO_2 is well below the contrast detection threshold of the human eye. The mean 24-hour solar input is 340 watts/m^2 . A widely accepted figure for excess solar input from anthropogenic emissions since pre-industrial times is about 1.6 watts/m^2 , Shepherd (2009), only 0.47 % of the input. Charlson et al (1987) give the fraction of suitable clouds as 0.18 of the sea surface. We need to increase their reflectivity by about 2.6% to reverse the damage done so far.

Figure 3 shows a set of 15 grey bars with equal contrast differences of 6.7%. Even with a properly adjusted computer screen or photo-printer it is quite difficult to detect which of any adjacent pair in the centre of the range is the brighter even though this difference is 2.5 times *more* than is needed to reverse the thermal effects of all human emissions since pre-industrial times. The task would be easier for close bars with sharp borders but harder for varied patterns with irregular edges.

A way must be found to enhance the contrast of clouds downwind of spray vessels. This can be done by taking a large number of satellite images, shifting them in the computer so that the spray source is in the same position in each, rotating them about the spray source to align all the mean wind directions and then averaging the pixel-by-pixel values of the entire set. This paper shows simulated results with mathematically brightened plume images and real satellite ones. Although Mathcad is a delightfully transparent environment its array handling tools proved very fast at image manipulation. Digital versions of these images and the MathCad worksheet can be made available.

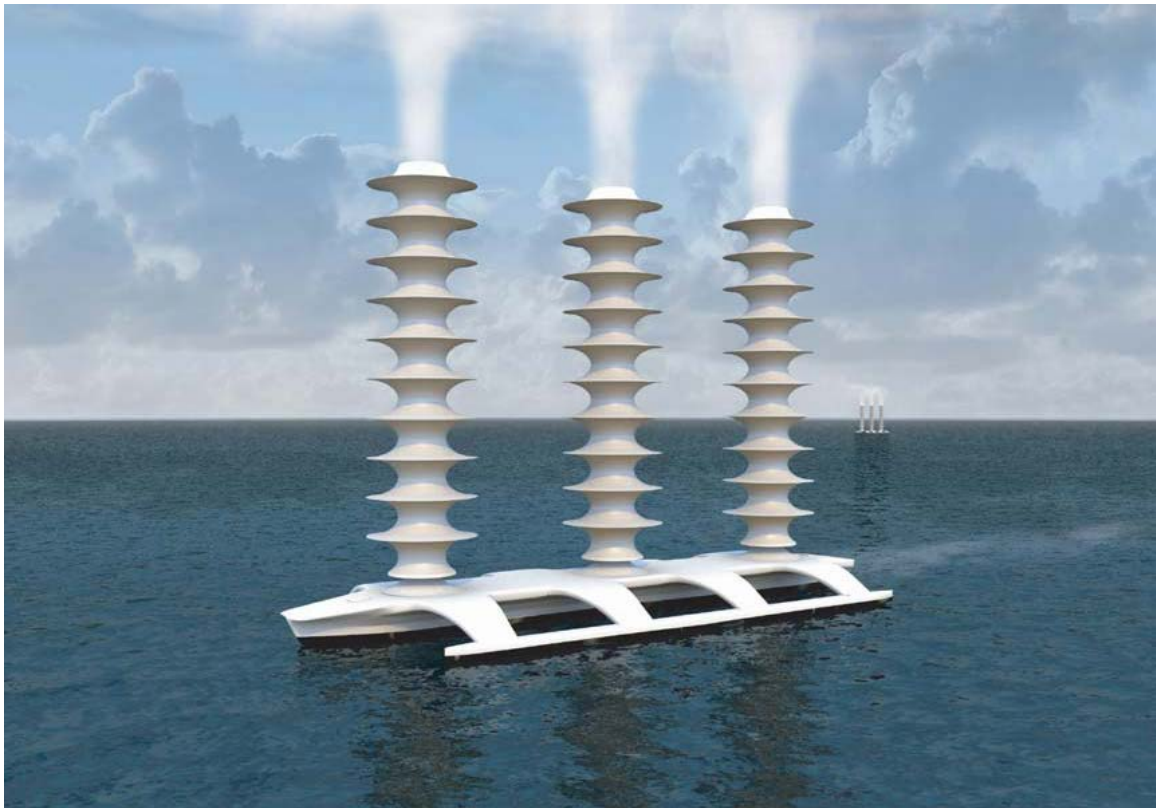


Figure 1. An artist's impression of a spray vessel driven by Flettner rotors with Thom fences. Turbines dragged through the water would produce energy to make 30 kg a second of 0.8 micron diameter spray. Artwork courtesy of John MacNeill.

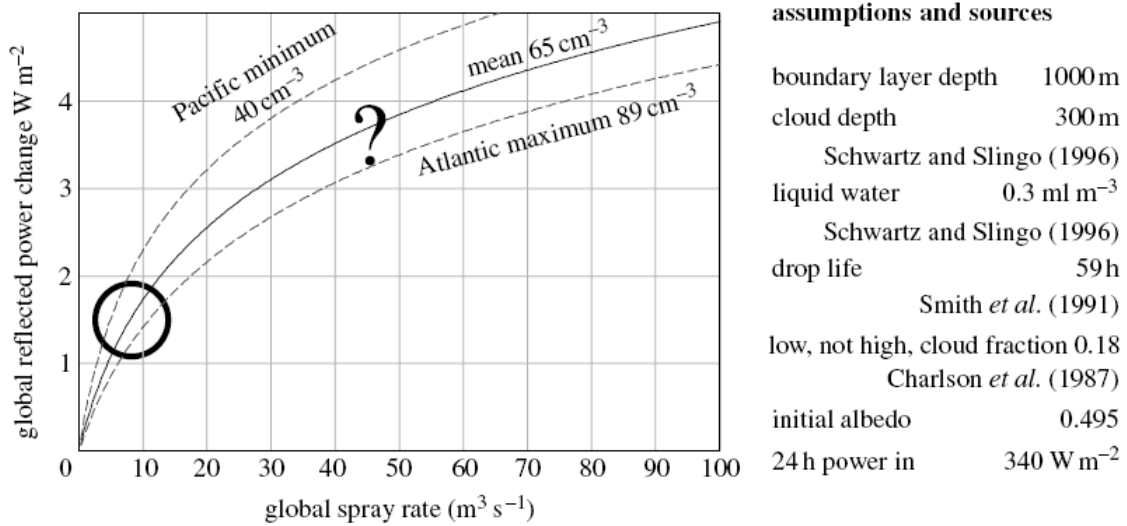


Figure 2. Global cooling as a function of spray rate for the assumptions in the table. The circle is the damage done since pre-industrial times. The query mark shows what might happen.



Figure 3. A 15-bar grey scale. It is hard to tell which of any adjacent pair is the brighter.

2. Cloud images.

Figure 4 is one of a set of 100 cloud images of the Pacific to the west of South America from the MODIS instrument on the Aqua satellite provided by Rob Wood and converted for use in a Mathcad worksheet. The wavelengths are the 0.52 to 0.72 micron band. The dynamic range of the images as downloaded has been stretched to extend from 0 for the darkest pixel to 255 for the brightest one. The mean value for this image is 164.7. In order to avoid future over-ranging, the brightness of all pixels was reduced by a factor of 0.8. The images cover 10 to 30 degrees south latitude in 491 pixels and so each pixel represents 4.53 kilometres. Linear cloud features which may be the result of ship emission are observed at 0.25 of the width from the left of the image and 0.1 down.

For this demonstration it is assumed that the wind is from due north rather than the usual prevailing direction to distinguish this mathematical simulation from genuine ship tracks, American Meteorological Society (2000), and any future images with the correct wind direction.

If the concentration of nuclei follows a Gaussian distribution the divergence of a plume can be described by the angle between the standard deviation and the mean line of the plume. For a constant wind direction this angle is typically 1 degree over the sea and 3 degrees over land. We can cater for veering and backing of the wind direction, or our own errors in estimating it, by increasing the diversion angle.

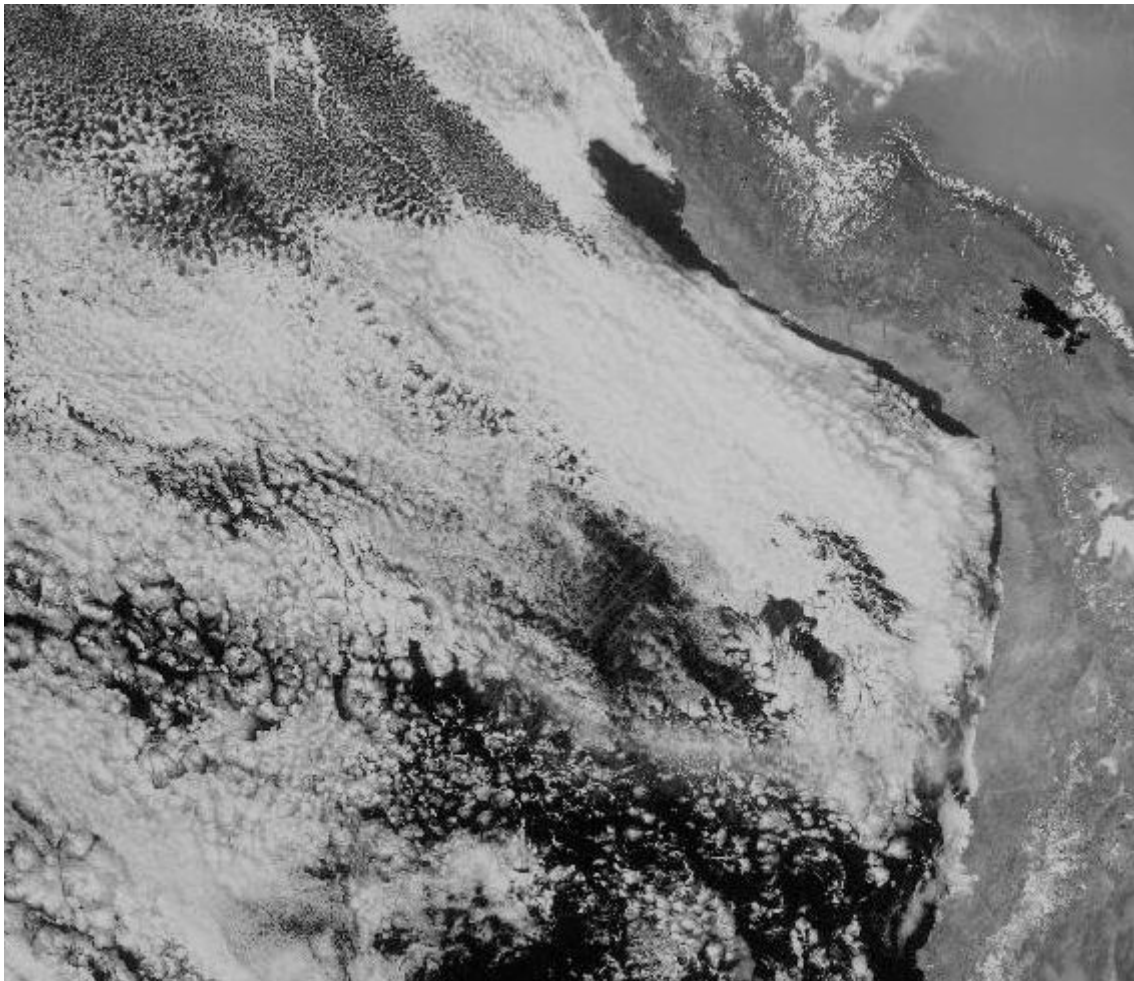


Figure 4. One of a set of 100 MODIS satellite images of cloud patterns on the Pacific coast of South America supplied by Rob Wood as part of the 2008 VOCALS study.

3. Effects of spray

The first assumptions for the reflectivity change might be regarded as somewhat conservative by albedo control enthusiasts and are given below in table 1. Suggestions for other inputs would be welcome and the resulting images can be produced very quickly.

Table 1. Conservative assumptions

Spray rate from one spray generator	0.01 m ³ /sec as 0.8 micron diam. = 3.73 x 10 ¹⁶ /sec
Wind speed	8 m/sec
Rise time to boundary layer	4 hours
Infant survival rate	0.5
Half life	24 hours (The shortest suggested so far)
Initial CCN concentration	89/cm ³ (Bennartz Atlantic maximum)
Boundary layer depth	1000 m
Plume standard deviation divergence half-angles	1, 2, 5, 10 degrees
Source positions as a fraction of image width	0.05 ,0.15, 0.25, 0.4
Liquid water content in clouds	0.3 gm/m ³

Figure 5 shows graphs of the resulting concentration of cloud condensation nuclei for the four chosen divergence angles at east-west transects placed at 0.1 (red) and 0.3 (blue) of the vertical size of the image down from the top. The effects of plume widening are clear. The widest plume at the 0.3 transect is barely detectable. Work on the correlation of these signals with original and spray-enhanced images is in progress with the aim of computer-aided pattern recognition.

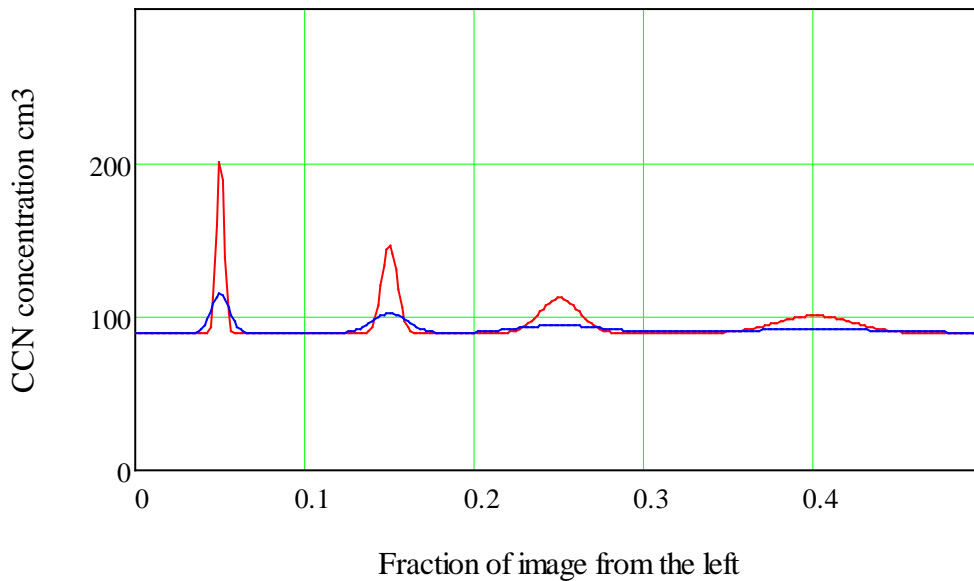


Figure 5. Graphs of cloud condensation nuclei concentration along transects of the plumes.

In figure 6 we apply the reflectivity change to an even-brightness field in which the initial pixel value was set to 128 out of the 255 maximum. After the reflectivity increase, the maximum brightness is 144.5 and three of the four plumes can be detected against the constant background.

In figure 7 we have subtracted 127 from each pixel, multiplied each by 50 and then reduced any value over 255 down to 255. This has the effect of adjusting what photographers call the gamma curve of an image and shows how plumes blend with one another. A similar experiment shows that a pair of two-dimensional Gaussian plumes with 1 degree dispersion half-angles merge to an even concentration at a distance 30 times their separation and that with a 3-degree half angle the merge distance is 10 times the source separation.



Figure 6. Three plumes are just detectable against an even background.



Figure 7. The effect of gamma change on figure 6.

Figure 8 shows the image of figure 4 with the pixel reflectivity increased by the amount suggested by Schwarz and Slingo (1996) in their account of the Twomey results. For a wide range of conditions the reflectivity change is within 10% of:

$$\Delta\text{Ref} = \frac{1}{12} \cdot \ln\left(\frac{\text{NewCCN} + \text{OldCCN}}{\text{OldCCN}}\right)$$

V

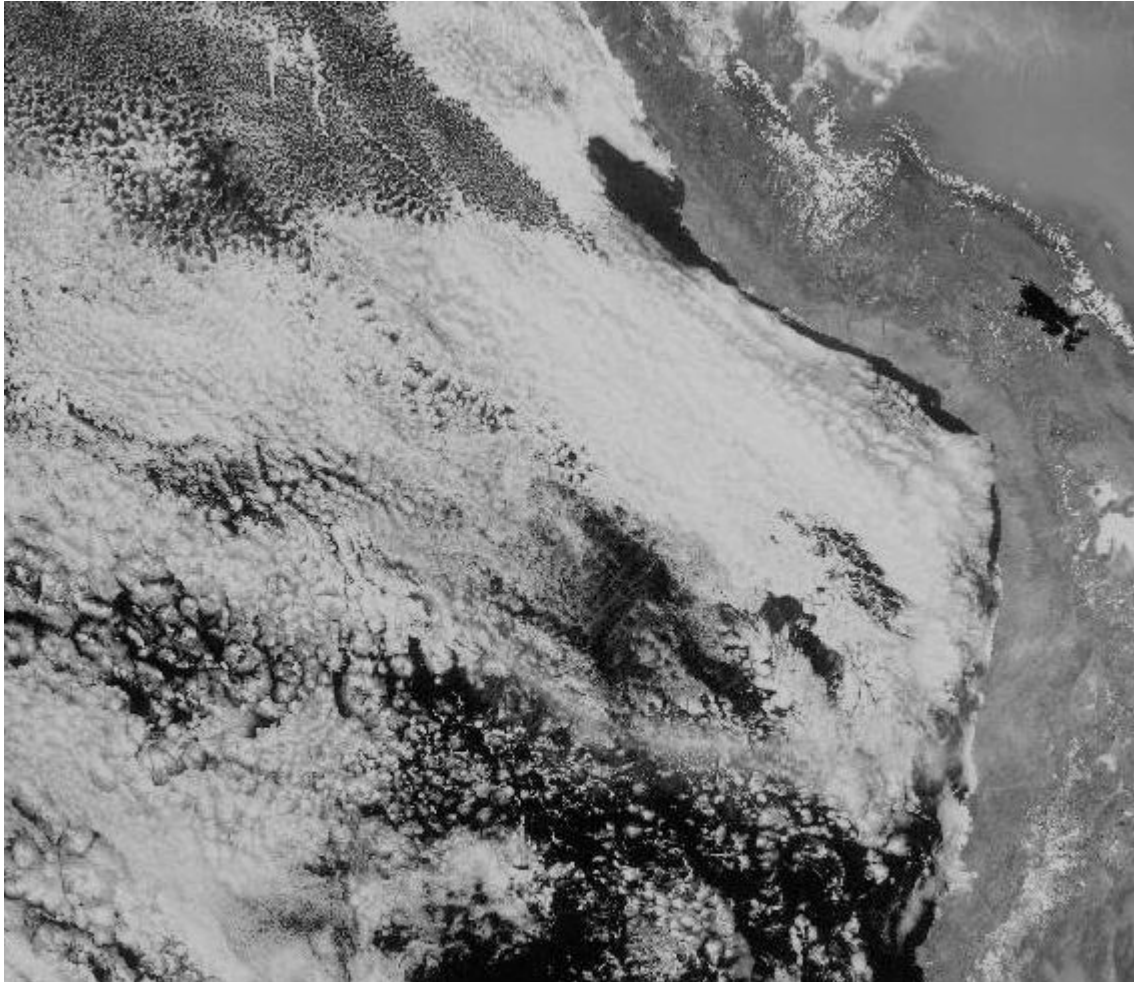


Figure 8. The enhancement of reflectivity for the assumptions given in table 1 is not easily detected.

A non-technical decision-maker would need a great deal of convincing to agree that there is any sign of the 1-degree streak below the V at the top left of the image. Any error in the rotation of the wind direction would make this even harder.

Figure 9 shows graphs of the brightness across the 0.3 transect over the left half of the image before and after spray. Several of the parameters needed to calculate the effectiveness of spraying will show a similar range of statistical variation. Differences between the graphs are not obvious.

Only by plotting them together and zooming in on the affected region, as in figure 10, can we see the differences. Just as with the difficulty of stepping into the same river twice, it would not be possible to photograph exactly the same clouds before and after treatment, Heraclitus (504 BC).

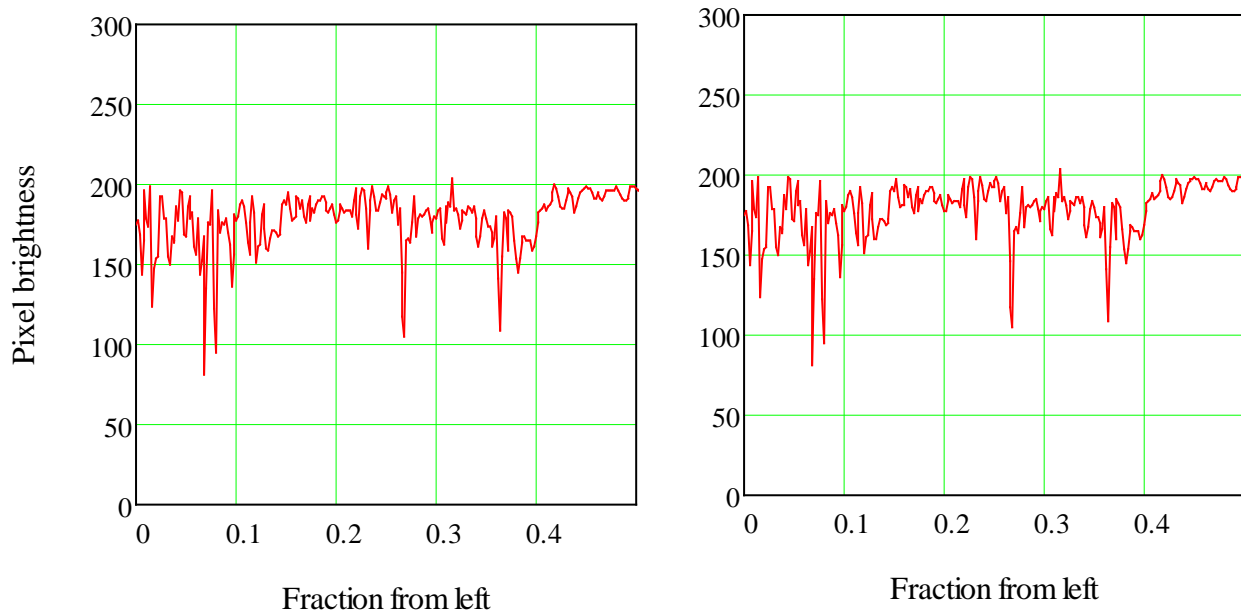


Figure 9. The brightness transects at 0.3 of the vertical fraction of the left half of figure 8 are very similar.

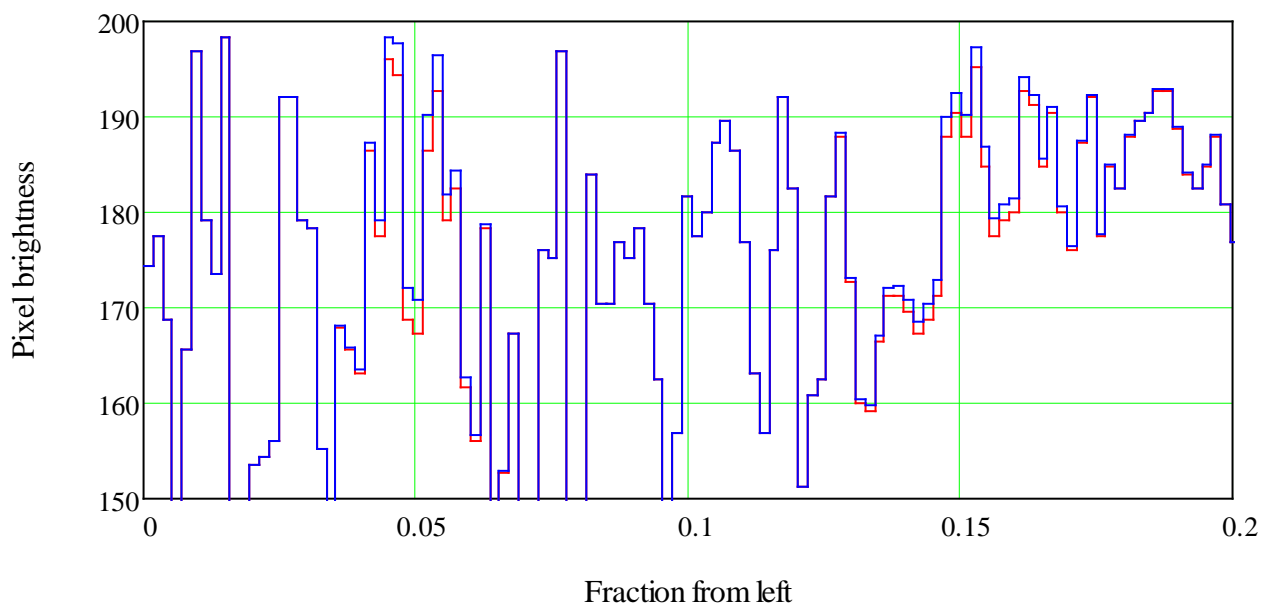


Figure 10. Zooming in on the superimposed pair shows the differences of the same image before (red) and after spray (blue). This would not of course be possible with changing cloud fields. No matter how good the instrumentation we have a problem detecting changes smaller than natural variations.

In figure 11 we assume that the translation of source position and rotation to align wind directions have both taken place accurately and that we have then averaged 100 real satellite images after enhancement by the new concentration of nuclei. We can see that the uncorrelated cloud images are converging to a middle grey to suppress the camouflage effect of random patterns. Two plumes are detectable and the third is faintly suggested.

In figure 12 we again adjust the gamma curve. A brightness value of 130 has been subtracted from each pixel and the resulting value multiplied by 3.5. The values were chosen as a compromise between contrast increase and over-ranging or under-ranging the 0 to 255 brightness scale. This would be more effective the greater the number of images used in the averaging process.

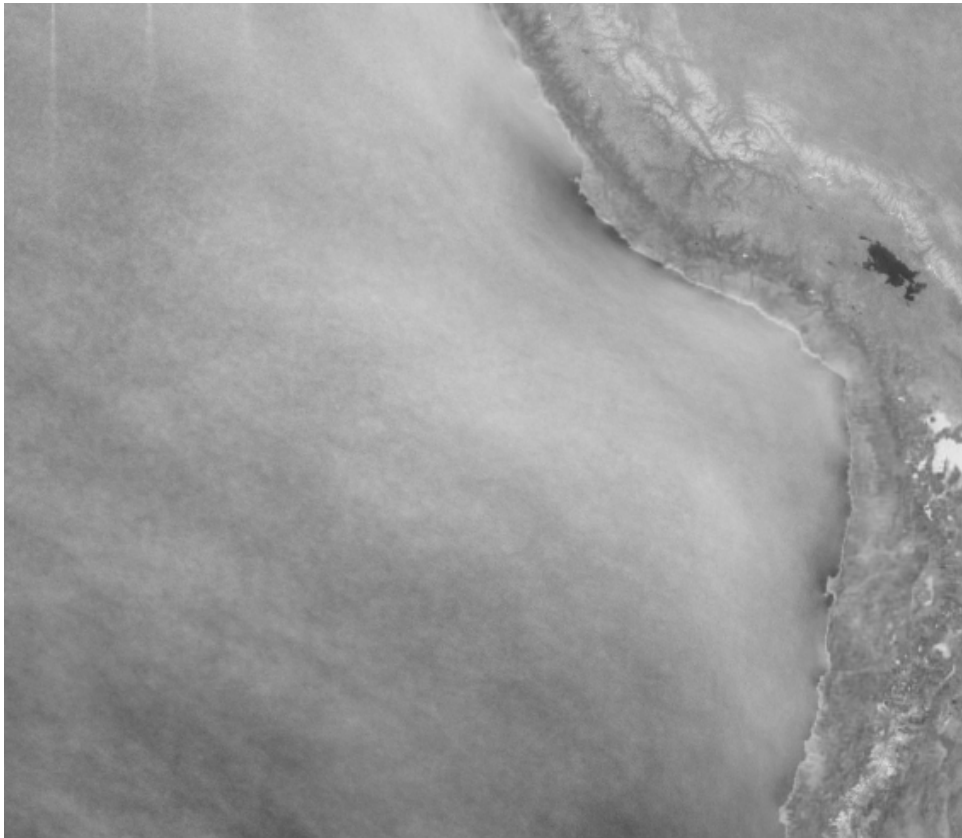


Figure 11. Plumes become just visible if 100 uncorrelated images are averaged.

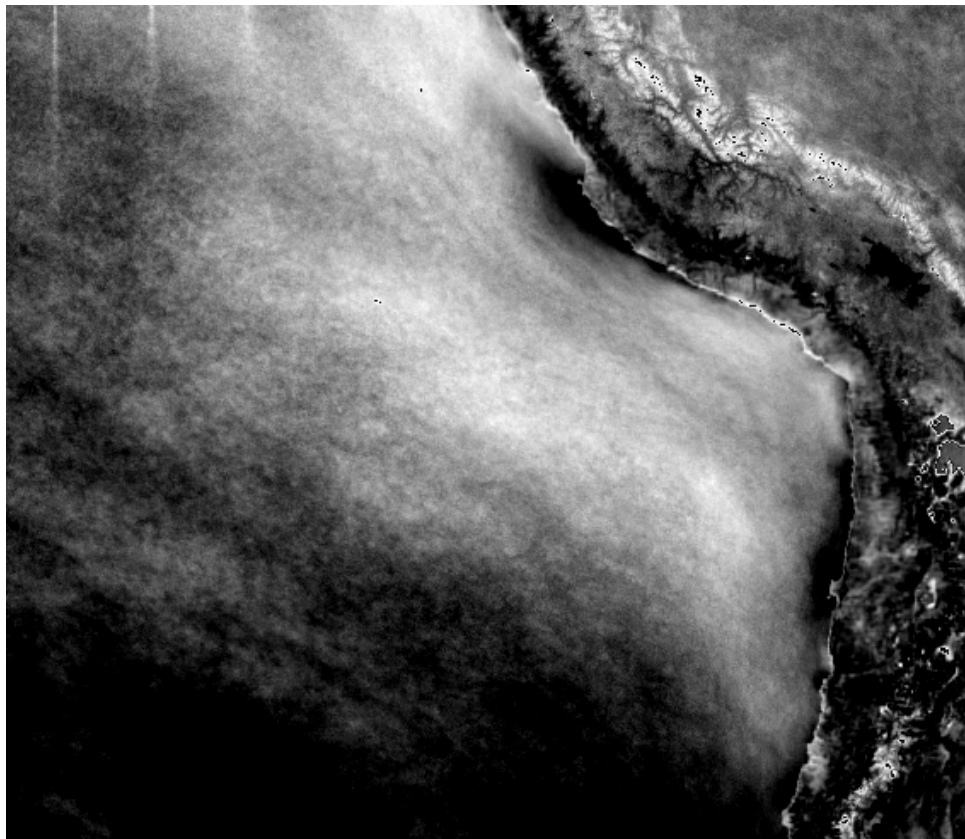


Figure 12. The effect of gamma correction on figure 11.

Next we make more optimistic assumptions as in table 2. The spray rate has been raised to 0.03 m³/sec, appropriate for the three spray canisters aboard a spray vessel. The wind speed has been reduced to 6 m/sec. It is assumed that, because the vertical component of turbulence velocity vanishes at the water surface, the infant survival fraction is unity. The half life of nuclei is increased to the 59 hour value suggested by Smith (1991) and confirmed for a 0.8 micron spray diameter by Hoppel (2002). These give table 2 and the resulting image of figure 15.

Table 2. Less severe assumptions than those of table 1.

Spray rate up from 0.01 m ³ /sec	0.03 m ³ /sec as 0.8 micron diam. = 1.12 x 10 ¹⁷ /sec
Wind speed down from 8 m/sec	6 m/sec
Rise time to boundary layer unchanged	4 hours
Infant survival rate up from 0.5	1
Half life up from 24 hours	59 hours (Smith and Hoppel)
Initial CCN concentration reduced from 89/cm ³	65/cm ³ (mean of Bennartz)
Boundary layer depth	1000 m
Plume standard deviation divergence half angles	1, 2, 5, 10 degrees
Source positions as a fraction of image width	0.05, 0.15, 0.25, 0.4
Liquid water content	0.3 gm/m ³

With the more optimistic assumptions three plumes are clearly shown and the fourth indicated with no need for gamma adjustments. If a subtraction of 110 followed by a multiplication by 2.1 for each pixel had been applied the result would be figure 16.

4. Implications for planning field experiments.

While the most urgent need for albedo control might be from land-based sources on the Faeroe Islands aimed at saving the Arctic ice cover, the air in the southern Pacific is cleanest and would give the technology its best chance of success. The first objective should be to prove whether or not the idea works at all. The second should be to determine the situations for which it does work and those for which it does not, Wood (2007). The third should be to measure values of all the parameters that govern the size of the effect so that the computer models can be refined. The two last require spraying in a wide range of conditions. Given the importance of temperatures on each side of the Pacific with regard to the balance between el Nino and la Nina events it seems desirable to cover both sides with a wide range of latitudes from the equator to the Antarctic ice limit.

Lima in Peru is at longitude 77 degrees 15 minutes west. The west coast of South America has been the subject of extensive measurements for the recent VOCALS project and so offers a rich data base. A cruise might begin at Lima and go due south along the 80 degree meridian to as far past latitude 60 south as we dare, through the VOCALS area. This single passage might be enough to meet Objective One. The spray vessel would then steer a zig-zag course starting NNW towards the equator to longitude 100 west, then SbW back to 60 south 120 west and so on to the equator at 140 west. It would take eight such sweeps to reach Micronesia with a small deviation round new Zealand, a total distance of nearly 55,000 km. At a speed of 6 metres per second this will take 106 days. We want the centre of the cruise to be in the southern mid-summer and so we should work from the end of April to mid-August.

The rotation period of the Aqua satellite is 99 minutes. The width of the MODIS swath is 2300 km or 20.7 degrees wide at the equator. In 99 minutes the earth rotates 24.75 degrees and if the vessel is less than about 32 degrees from the equator it may be missed on some days while swaths will overlap at higher latitudes. Its orbit is sun-synchronous and it crosses the equator at 1:30 pm local time. Aqua will therefore be over the middle of a leg at 30 degrees south latitude 8.25 minutes earlier. With 14.5 orbits a day we should have good illumination on, say, 4 of them but it would be safe to assume less than one usable image of the spray plume a day from MODIS. Access to data from MTSAT is being investigated.

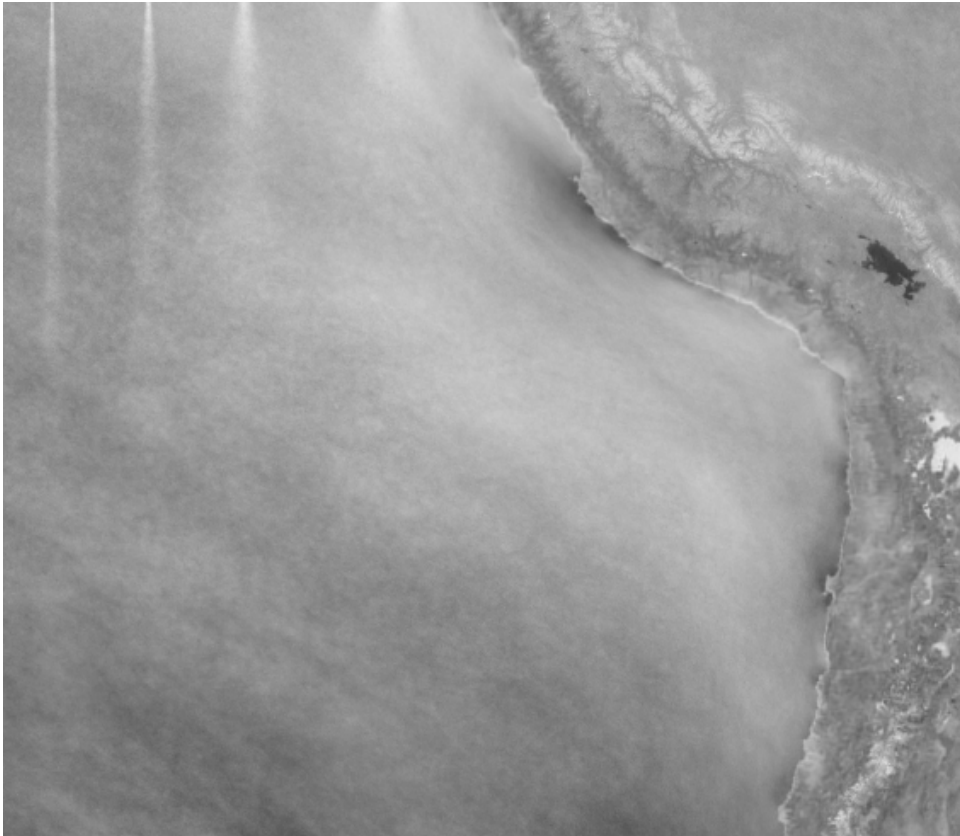


Figure 15. The result of averaging for less severe assumptions given in table 2.

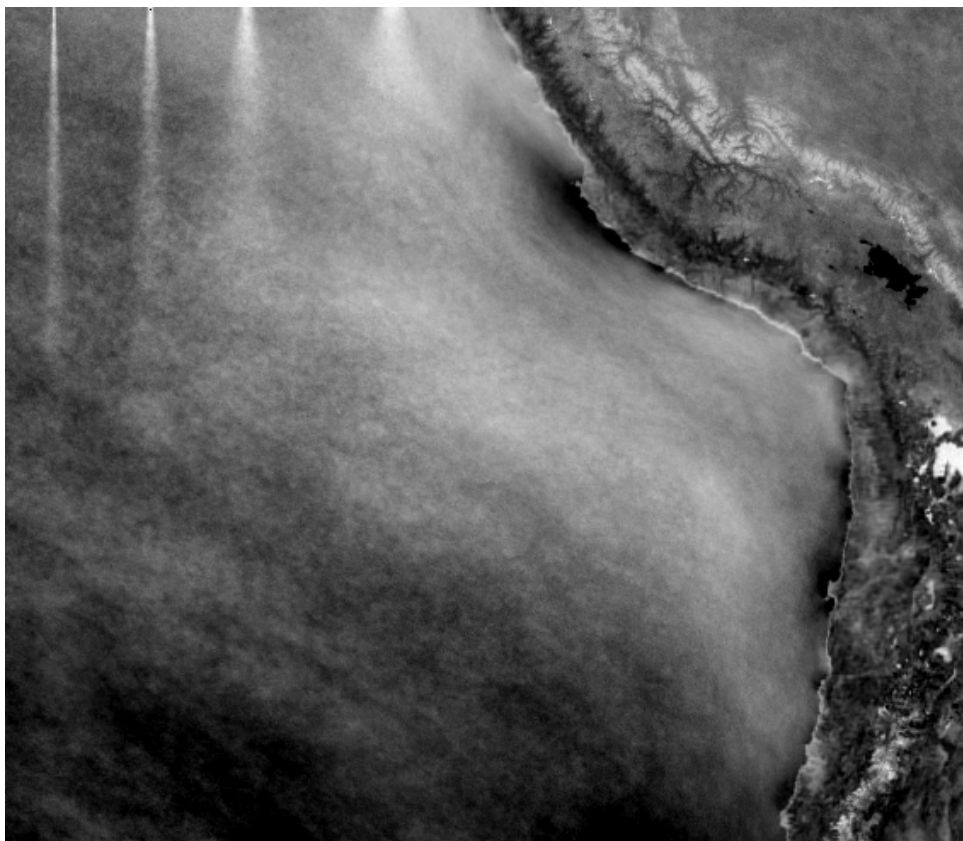


Figure 16. Gamma enhancement of figure 16 may not be necessary to see all four plumes.

The difference between figure 11 and figure 15 shows that we should try to release at least 0.03 kg/sec unless we can get other advice about nucleus half life, infant drop survival and initial concentration of condensation nuclei. If these do show that there is a chance of better detection then the cruise could be shortened to four zig-zags. In some situations it might be useful for the ship to take a course and speed which is the same as that of the wind at the cloud top. This would concentrate spray in an expanding circular patch. Unfortunately few ships have enough speed to travel at cloud top velocities.

Research vessels cost between \$20,000 and \$30,000 a day and only sailing ships could travel such distances without refuelling. At this rate the full eight sweeps would cost over \$3 million. It would be desirable to combine the cruise with the collection of other data.

5. Conclusions

- The cloud contrast change needed to save human existence is below the contrast detection threshold of the human eye so that special techniques must be designed to show a non-technical decision-maker whether or not the system will work.
- Computer shifting, rotating, averaging and gamma adjustment can allow an increase in contrast.
- Uncertainties about wind direction are serious but can be modelled by increasing the assumed half angle of plume divergence.
- It is possible that a single passage across the VOCALS test area could give a positive result but a longer cruise would allow the collection of data to refine inputs for global climate models.

6. Acknowledgments.

I am particularly grateful to Rob Wood for the supply of the VOCALS images and advice on their use and also to the authors of MathCad which, as usual, prevents me from making many foolish mistakes.

References

- American Meteorological Society. 2000. Special issue on ship tracks. From <http://ams.allenpress.com/perlserv/?request=get-toc&issn=1520-0469&volume=57&issue=16>
- Bennartz, R. 2007. Global assessment of marine boundary layer cloud droplet number concentration from satellite. *Journal of Geophysical Research*, **112**, 12, D02201, doi:10.1029/2006JD007547.
- Charlson R.J., Lovelock J.E., Andreae M.O., Warren S.G.. 1987. Oceanic Phytoplankton, atmospheric sulphur, cloud albedo and climate. *Nature* **236** pp. 655-661
- Heraclitus. 504 BC. On nature. Ephesus press.
- Hoppel, W. A. Frick, G. M. Fitzgerald, J. W. 2002. Surface Ocean function for sea-salt aerosol dry deposition to the ocean surface. *J.Geophysical Research*, vol 107 no D19 doi:10.1029/2001JD002014.
- Latham, J. 1990. Control of global warming. *Nature* **347** pp 339-340.
- Latham, J., Rasch, P., Chen, C-C, Kettles, L., Gadian, A., Gettleman, A., Morrison, H., and Bower, K., Choulaten, T 2008. Global temperature stabilization via controlled albedo enhancement of low-level maritime clouds, *Phil Trans Roy Soc.A* Doi:10.1098/rsta.2008.0137.
- Salter S.H., Latham, J. Sortino, G. 2008 Sea-going hardware for the cloud albedo method of reversing global warming. *Phil.Trans.Roy. Soc. A.* Doi:10.1098/rsta.2008.0136
- Schwartz, S. E. & Slingo, A. 1996. Enhanced shortwave radiative forcing due to anthropogenic aerosols. In *Clouds Chemistry and Climate* (Crutzen and Ramanathan eds.) pp 191-236 Springer Heidelberg.
- Shepherd J. *Geoengineering the climate*. 2009 pp2-3. The Royal Society London.
- Smith, M. H., Park, P.M & Consterdine, I.E. 1991. North Atlantic aerosol remote concentrations measures at a Hebridean coastal site. *Atmospheric Environment* **25A**, no3/4 pp 547-555.
- Twomey, S., 1977. Influence of pollution on the short-wave albedo of clouds. *J. Atmos. Science.*, **34**, 1149-1152.
- Wood, R. 2007. Cancellation of aerosol effects in marine stratocumulus through cloud thinning. *Journal of the Atmospheric Sciences*. **64** pp 2657-2669.